www.sciencemag.org/cgi/content/full/1153894/DC1

Supporting Online Material for

Elevation Changes in Antarctica Mainly Determined by Accumulation Variability

Michiel M. Helsen,* Michiel R. van den Broeke, Roderik S. W. van de Wal,
Willem Jan van de Berg, Erik van Meijgaard, Curt H. Davis, Yonghong Li, Ian Goodwin

*To whom correspondence should be addressed. E-mail: m.m.helsen@uu.nl

Published 29 May 2008 on *Science* Express
DOI: 10.1126/science.1153894

This PDF file includes:

Supporting Online Material

Firn densification model

The firn densification model described by (*13*) is used as the model to simulate firn depth changes over the grounded Antarctic ice sheet. We followed their approach, and refer to their work for the basic equations.

For a successful application to Antarctica, a parameterization was needed for the empirical factor β (*13, S1*), which scales the relative importance of grain growth (K_{0G}) in the total densification rate (K_{rate}), by:

$$K_{rate}(T) = \beta K_{0G}(T)\exp\left(-\frac{E(T)}{RT}\right) \qquad (1)$$

where E is the activation energy, R is the gas constant and T is temperature.

(*S1*) proposed an expression of β as a function of annual mean surface temperature ($\overline{T}_s$), based on a comparison with eight Greenland sites. The range of $\overline{T}_s$ over these sites is not large enough to cover conditions for Antarctica. Moreover, at higher temperatures, this relation predicts unrealistic (negative) values of β. Therefore, we established a new β-$\overline{T}_s$ relation for Antarctica (Fig. S1), by using 41 observations of the approximately pore close-off depth (depth of the 830 kg m^{-3} density level) as the depth to which the firn densification model is tuned, by varying β until agreement with the observed pore close-off depth is reached. The resulting distribution of β is shown in Fig. S2.

Another parameter in the densification model that can be adjusted to obtain agreement with field observations is the density of snow that accumulates at the surface, ρ_s. Here, ρ_s

is estimated using an empirical relation that predicts ρ_s from annual mean values of surface temperature, wind speed and accumulation (*S2*). We applied a slope correction of:

$$\rho_{s,corr} = -154.91 + 1.4266\rho_{s,Kaspers} \qquad (2)$$

to this relation to obtain realistic values in more agreement with observations (based on a data set of 50 locations), and used a maximum value of ρ_s = 470 kg m^{-3}, since no higher values are observed (Fig. S3).

Firn depth variability

The equation that describes surface height changes (in m yr^{-1}) on an ice sheet over time is:

$$\frac{dH}{dt} = \frac{A - M}{\rho_{surf}} - v_{fc} - v_{ice} - v_{GIA} \qquad (3)$$

Where A is accumulation (in kg m^{-2} yr^{-1}) and is calculated as the sum of solid precipitation (P_{sol}) and sublimation (Su), v_{fc} is the vertical velocity (in m yr^{-1}) of the surface due to firn compaction, v_{ice} is the vertical velocity of the ice, v_{GIA} is the vertical velocity of the underlying bedrock due to glacial isostatic adjustment and M is the surface melt. Here, observed (ERS-2) dH/dt values are corrected for the effect of v_{GIA} (*10*). v_{fc} can be described by the integral of the rate of densification below the surface (z=0):

$$v_{fc}(0,t) = \int_{z_{ice}}^{0} \frac{1}{\rho(z)} \frac{d\rho(z)}{dt} dz \qquad (4)$$

Hence, 'firn depth' is defined as the depth from the ice sheet surface to the depth where the density reaches the ice density (ρ_i=917 kg m^{-3}). However, here we assume that the vertical velocity of the lowest model level ($v_{fc,1}$) is in equilibrium with the average annual accumulation rate (A_b), such that it balances the vertical ice velocity:

$$v_{fc,1} = \frac{\rho_{ice}}{\rho_1} v_{ice} = \frac{A_b}{\rho_1} \qquad (5)$$

Therefore, reported changes in firn depth are due to accumulation, sublimation and temperature-driven densification of the simulated (upper) part of the total firn column. We have performed 2 different model experiments. Firstly, we simulated firn depth variability using annual accumulation values from ice core records (Fig. 1a and b in the manuscript), Secondly, the firn depth variability was simulated for the entire Antarctic grounded ice sheet, using data from a calibrated regional climate model, over the period 1980-2004.

Model input for long-term firn depth change runs

The accumulation records shown in Fig. 1 in the manuscript from Wilkes Land (WL) and West Antarctica are stacked records. For WL, we used 3 out of 4 available records (GD03, GD06, GD15, *16*), and stacked them by simply averaging annual accumulation. We decided not to use GD09 for the stack, because it has been shown that accumulation at this site is anomalous to the general accumulation pattern in this region (*16*), probably owing to snowdrift.

For West Antarctica, a total of 12 accumulation records are available (*18*), from a large area. From these 12 records, 4 cores are located reasonably close to each other and with sufficient length (00-1, 00-4, 00-5, RIDS-A), and these were stacked to reconstruct accumulation of the specific area that shows a negative dH/dt_{corr} trend (Fig. 2a in the manuscript). It should be noted that stacking the records has removed part of the variability in the accumulation time series.

The ice core records did not include the entire period of ERS-2 radar altimetry measurements (1995-2003). Thus, we extended these records with accumulation from the regional climate model (see below). To couple the accumulation records from ice cores with the accumulation from the regional climate model, overlapping periods were used to scale the accumulation from the regional climate model, to avoid unrealistic jumps in accumulation, and thus in H(t) time-series. Furthermore, an average annual temperature cycle (6 h resolution) was calculated from the regional climate data, and applied to all years covered by the ice core records. The latter is important as densification depends non-linearly on temperature.

Model input for the 1980-2004 firn depth change runs over the grounded ice sheet

The firn model is applied to the entire grounded Antarctic ice sheet, on a ~55 km resolution, using 6-hourly values of T_s, P_{sol} and Su from calibrated output of a regional atmospheric climate model over the period 1980-2004 (RACMO2/ANT, *20*). RACMO2/ANT is forced on its lateral boundaries using European Centre for Medium-Range Weather Forecasts (ECMWF) reanalysis (ERA-40) and operational analyses. Using this input, a heat diffusion equation for firn (*S3*) and the firn densification equation are numerically solved using the semi-implicit Crank-Nicolson scheme. The maximum snow layer thickness is 10 cm (progressively thinning downward with increasing density) and the time-step is 3 h. In contrast to (*9*), we did not incorporate melt or vapour diffusion effects on the densification, as these effects are small on the dH/dt results for the grounded part of Antarctica.

The initial state of the firn model is reached by first assuming a steady state firn density profile over the first 15 m of firn, and then running the model twice over the available 25 yr of inputdata, to allow the density profile to come in equilibrium with the time-dependent meteorological input during 50 yr. Then the 25 yr reference run is performed, over the period 1980-2004.

As an example of firn depth time-series, Fig. S4 shows simulated H(t) results for Law Dome, coastal East Antarctica. During the 1980s the surface elevation stays relatively constant, but during the early 1990s a surface height increase is caused by a 3 yr period with a positive accumulation anomaly. Then, a decreasing trend is visible after 1997, which is the result of a 4 yr period with a negative accumulation anomaly. The positive anomaly in temperature is not large enough to have an appreciable effect in the elevation time series, but note the distinct influence of the seasonal temperature cycle on the firn densification rate: a seasonal oscillation in the elevation time-series is apparent, with an average amplitude of ~20 cm for this location. From 1995 to 2003 a negative dH/dt of -15 cm y^{-1} can be identified. These values are plotted over the entire grounded ice sheet in Fig. 2a of the manuscript.

Sensitivity of results to variations in accumulation and temperature

To illustrate the dominance of the accumulation anomaly over the temperature anomaly in forcing dH/dt, both patterns are plotted in Fig. S5a and c. The patterns resemble each other, with positive accumulation anomalies being associated with higher than average temperatures. On short time-scales (i.e. days), there is a strong correlation between temperature and accumulation, resulting from warm moist air masses that bring precipitation to the Antarctic continent (e.g. *S4*). Fig. S5a and c show that there is still a weak correlation between accumulation and temperature over the 1995-2003 period. A comparison with Fig. 2a from the manuscript clearly illustrates that the pattern of firn depth changes closely resembles the accumulation anomaly pattern.

Two additional model runs were performed keeping either the temperature (Fig. S5b) or the accumulation rate (Fig. S5d) constant on their average value over the entire simulated period (1980-2004). These sensitivity runs demonstrate the large influence of accumulation, and furthermore show that temperature fluctuations have less impact in elevation change trends over inland Antarctica.

Low temperatures that prevail in Antarctica can explain the latter effect. Even though densification rate is strongly dependent on temperature, perturbations of the temperature only have large effects when the temperature becomes close to zero for at least part of the year, which is barely the case in Antarctica. These results are in agreement with (*S1*), who showed that a cooling over East Antarctica resulted in a temperature-driven increase of the surface elevation, especially in the coastal area of WL. However, the magnitude of the temperature effect is much smaller then the effect of a decreased accumulation rate in the same period, which results in a net decrease in firn depth in WL in our simulation.

In the previous paragraph it was explained how the initial state of the firn density (at 1 January 1980) is reached. The influence of this approach on our results may be that accumulation anomalies occurring in the last few years of the 50 y spin-up may have an effect on the first few years of the reference run. To test this influence, we used accumulation data over the period 1957-1980 based on ice core data and ERA-40 reanalysis data (*3*) as alternative input to reach the initial state of the firn density profile at the start of the simulation. To account for systematic differences between the two input data sets, and thus to avoid a sudden jump in the H(t) time series, we used an overlapping period (1980-1994) to scale the ice core/reanalysis data set with RACMO2/ANT accumulation, and used the mean annual temperature cycle for the simulation prior to 1980. The results from this run (not shown) are almost identical to the reference run, which show little dependence on initial conditions.

Correcting the ERS-2 data for 1995-2003 firn depth effects

Observed dH/dt values from ERS-2 (corrected for postglacial rebound) are resampled to obtain values on the same grid as RACMO2/ANT, which enables comparison and correction of the observations. The observed dH/dt pattern from ERS-2 is shown in Fig. S6. The corrected elevation change values (dH/dt_{corr}, Fig. 2b in the manuscript) are obtained by subtracting the simulated values (Fig. 2a in the manuscript) from the observations (Fig. S6).

If dH/dt_{corr}=0, then all observed elevation changes could be attributed to (simulated) accumulation of snow and firn densification. This also means that the prescribed vertical ice velocity is accurate. However, if there is a difference between simulated and observed dH/dt values, this can be either due to differences between simulated and actual meteorology during the simulated period or to an imbalance between the simulated and actual vertical velocity of the original firn surface (layer of 1 January 1980). We are confident that our simulated meteorology is of adequate quality, so we attribute differences between observed and simulated dH/dt values to a difference between simulated and actual vertical velocity of the 1980 firn surface, which is in essence equal to an imbalance between $A_{80\text{-}04}$ and A_b (the latter dictates vertical velocity of the firn under the 1980 layer). When $A_{80\text{-}04} < A_b$, simulated vertical velocity of the 1980 firn layer will be lower than the actual velocity, which results in a higher simulated dH/dt value than observed. This in turn yields a negative value of dH/dt_{corr}. Hence, dH/dt_{corr} is a measure of the deviation of $A_{80\text{-}04}$ compared to A_b.

From elevation changes to mass changes

In evaluating overall mass change, a distinction is again made between 'short-term' mass changes due to the 1995-2003 accumulation anomaly relative to $A_{80\text{-}04}$, mass change estimates resulting from the original ERS-2 data and mass changes due to an imbalance between $A_{80\text{-}04}$ and A_b (Fig. S7).

To calculate mass changes from elevation changes, the following equation has been used:

$$\frac{dM}{dt} = \frac{dH}{dt} \cdot Ar_g \cdot \rho_* \qquad (6)$$

where Ar_g is the area of the grounded ice for the grid point, and ρ_* is the density of firn/ice. When changes in accumulation are expected responsible for volume changes, surface snow density (ρ_s) is commonly used for ρ_* (with a typical value of ρ_s=350 kg m^{-3}, *10, 11*), whereas the density of ice (ρ_i=917 kg m^{-3}) is used in areas where ice-dynamically induced elevation changes are suspected to be the key process. Mass estimates from uncorrected ERS-2 observations (Fig. S7) are thus produced using ρ_s for all basins except 14, 15, 16, and 19, where ρ_i is used.

However, here we have accounted for the 1980-2004 accumulation and densification effects for the corrected ERS-2 estimates, and these corrected dH/dt values are due to variations in accumulation rate with a timescale larger than 25 yr. Therefore, using ρ_s

leads to an underestimate of dM/dt values corrected for 1995-2003 firn depth effects, while ρ_i leads to an overestimate. Although we have simulated density profiles, we can only have confidence in the firn density over the depths that consist of accumulated snow from the period 1980-2004. For the estimate of mass changes due to long-term accumulation imbalances, we use the density ρ_1 (Eq. 5), which is the density of the lowest simulated firn layer (hence the snow that accumulated at 1 January 1980), averaged over the period of satellite observation (1995-2003). Values of ρ_1 range between 324 kg m^3 for cold, low accumulation areas in the interior to ρ_i (917 kg m^{-3}) for a few warm, high accumulation grid points near the coast. Using ρ_1 for the volume-mass conversion produces a conservative mass change estimate, since in principle the effective density can be any value between ρ_1 and ρ_i, depending on which time scale the accumulation rate change occurred. Nevertheless, it produces higher mass estimates then using ρ_s, which is commonly done in volume-mass conversion for dH/dt data. For drainage basins where we suspect that changing ice dynamics are responsible for elevation changes (basins 14, 15, 16 and 19 in Fig. 3 in the manuscript), we use ρ_i instead of ρ_1 in the calculation of dM/dt_{corr}. Values for the red bars in Fig. S7 are calculated by summing all dM/dt_{corr} values per drainage basin.

Mass budgets per drainage basin resulting from firn-depth-corrected ERS-2 data reveals an opposing pattern of mass gain (WL, PL) and mass loss (ASE, DML). Correcting for a positive firn depth anomaly in the ASE (produced by an accumulation anomaly of 10 ±1 Gt yr^{-1}) results in an enhanced ice mass loss of 20 Gt yr^{-1}, which yields a total ice mass loss of -71±9 Gt yr^{-1} for the ASE, which is an increase of the mass loss of 39% compared to the estimate without taking into account interannual variability in firn depth, and in agreement with (*7*) (Table S1). The mass losses from our analysis are possibly even underestimated in coastal areas, since elevation changes are generally largest in confined narrow glaciers, whereas ERS-2 track separation increases with decreasing latitude, which leads to poorer spatial sampling and hence to an underestimation of the maximum dH/dt signal.

Due to the extensive area in East Antarctica that shows an increase in elevation, the East Antarctic mass budget sums up to +87 ±9 Gt yr^{-1} (Table S1). This large positive estimate is attributed to a positive accumulation anomaly on a >25-yr time scale in basins 4-7.

For a sound comparison with previous mass balance estimates, we should add the 1995-2003 accumulation anomalies to the corrected ERS-2 mass change rates. This slightly reduces the East Antarctic mass budget (+84 ±10 Gt yr^{-1}), but brings the continental integrated mass budget to a total mass increase of +39 ±15 Gt yr^{-1}. Our large positive mass balance for East Antarctica is higher than earlier mass estimates resulting from the satellite-radar altimetry (*9-11*). This is due to the use of higher firn densities in our analysis, since we showed that the increase in ice sheet elevation is caused by an accumulation anomaly on a larger time scale than previously assumed. This large positive mass gain may also seem to be in disagreement with the insignificant trends in Antarctic snowfall in the last half century (3), but as showed in the main text (Fig. 1) thickening can occur without trends in accumulation, if recent accumulation is stepwise higher than A_b, which is also noticeable in reconstructed Antarctic accumulation records (4).

The large mass gain in WL also seems to conflict with (*7*), who used the same accumulation fields for mass input as this study. They find an approximate balance situation between $A_{80\text{-}04}$ and actual ice flux in WL. This apparent contradiction may be explained by processes acting on different time-scales: if accumulation was lower in the past, ice flow in the interior would still be too low to balance actual accumulation, causing thickening. A simultaneous acceleration of ice fluxes across the grounding line in WL would then suggest an apparent balance situation, whereas in fact two counteracting out-of-balance situations exist. Possible traces of such a situation are indeed identified in some major outflow glaciers in East Antarctica (S5), and can also be recognized in Fig. 2b where thinning of the lower reaches of some glaciers suggest acceleration (i.e. glaciers flowing into Cook ice shelf, Totten Glacier, Denman Glacier), surrounded by areas where ice sheet elevation change is dominated by increased accumulation.

Although our analysis concerns a different period than gravity-based estimates of mass change rates (GRACE), these also suggest mass gains of similar magnitude in East Antarctica (S6, S7). However, a discrepancy exist about the location of the mass gain; with GRACE estimates pointing towards a large mass increase in Enderby Land (S6, S7), while our results suggest a more eastward location.

Influence of small trends in accumulation rate

Although Antarctic accumulation rate does not show significant long-term trends over the period 1980-2004 (*15*), even small regional trends over this period can have an effect on the simulated firn depth changes over a shorter time frame, such as the ERS-2 observational period 1995-2003. To test this influence, we performed an additional simulation of Antarctic firn depth change using de-trended time-series (1980-2004) of P_{sol}, Su, and T. The pattern of firn depth changes in this de-trended run (DTRN, not shown) remains the same as in the control simulation (CTRL, Fig. 2a in the manuscript), but is has reduced the magnitude of the firn depth changes. The effect on the observed dH/dt values, corrected for the 1995-2003 firn depth trends, is that the ice sheet elevation increase in East Antarctica is somewhat reduced, but the magnitude of the declining ice sheet surface in West Antarctica is also reduced. In terms of resulting mass changes (dM/dt), the effect of using de-trended time-series of accumulation and temperature is plotted per drainage basin in Fig. S8. In WL (drainage basin 7), the removal of a (negative) trend in the 1980-2004 accumulation has strongly reduced the estimated positive mass change. However, the net effect of removing the 1980-2004 trends from the accumulation and temperature time series on the mass budget of the Antarctic grounded ice sheet is that the short-term accumulation anomaly over the period 1995-2003 decreases from +14±4 to +11±4 Gt yr^{-1}, and the long-term trend increases from +25±14 to +29±14 Gt yr^{-1}.

Error estimates

The overall error in simulated firn depth changes (Fig. 2a and 3), corrected elevation changes (Fig. 2b and 3) and accompanying mass changes per drainage basin (Fig. S7) is estimated from the root-sum-square of several independent error sources. These are calculated for the entire region of coverage and shown in Fig. S9.

The error in the trend of simulated firn depth over the period 1995-2003 (i.e. the error on the results in Fig. 2a in the manuscript) is influenced by different error sources, ranging from modelling errors to uncertainties in the input data. To quantify this error, 5 different error sources are investigated, i.e. the density of surface snow ($\sigma_{\rho s}$), the densification tuning parameter β (σ_{β}), the regression coefficient of the fit through the simulated dH time series (σ_{rc_dH}), the mean accumulation from input data (σ_{acc}) and trends in time series of accumulation over the period 1980-2004 (σ_{rc_acc}).

The RMS error from the parameterization of ρ_s is 23 kg m^{-3} (*S2*). Running the densification model using a 23 kg m^{-3} higher value for ρ_s assesses the effect of this error on the simulated firn depth change. The difference in simulated firn depth between the reference run and the model run using ρ_s+23 kg m^{-3} is regarded as the error from ρ_s ($\sigma_{\rho s}$, Fig. S9a). Generally, an increased value of ρ_s produces less pronounced elevation changes, with a factor of $\frac{\rho_s}{\rho_s + 23}$, and the differences are largest in areas with large firn depth changes.

The error introduced by the densification tuning parameter β is assessed by a model run using β=β+1.19, which is the RMS error from the correlation with temperature (Fig. S1). The difference between firn depth change from this run and the reference run is considered as the error from β (σ_β, Fig. S9b), and is only discernable in coastal areas.

The error in the linear fit through simulated firn depth time series is estimated using the standard error on the regression coefficient (σ_{rc_dH}, Fig. S9c) and is generally low. The highest value is in the order of 0.2 cm yr^{-1}.

Simulated firn depth results are dominated by the surface mass balance anomaly pattern. Therefore, time series of accumulation from RACMO2/ANT are a major error source. We estimate the error in accumulation time series on 10% of its annual mean value, and assess this influence on firn depth results using a 10% increased accumulation. The difference with the reference run (σ_{acc}, Fig. S9d) shows a comparable pattern as $\sigma_{\rho 0}$, since it is related to the magnitude of firn depth change. Furthermore, the influence of long-term (1980-2004) trends in the accumulation time series is incorporated in the error estimate of firn depth changes, by using the difference between the detrended run and the reference run (σ_{rc_acc}, Fig. S9e).

The resulting overall error in the trend of simulated firn depth over the period 1995-2003 ($\sigma_{firndepth}$, Fig. S9f) is dominated by uncertainty in trends of accumulation time series. Largest errors are typically ~10 cm yr^{-1} and are found in coastal areas, areas with large accumulation anomalies and where the 1980-2004 accumulation time series contain (small) trends. Note that it is likely that the errors are not independent, which causes an overestimation of the overall error estimate. The ratio of simulated firn depth trends with its error (Fig. S9g) shows that firn depth increases are significant in DML and in the ASE ($>2\sigma$), but not in the AP.

The error in ERS-2 observations is estimated from the least square line fit of the 8-yr time series. Since the ERS-2 data has a higher resolution than the RACMO2/ANT grid, the error estimates are resampled to the RACMO2/ANT grid using root-mean-squares of the ERS-2 data. To avoid an underestimation of the error, a value of $\sigma_{ERS\text{-}2}$=0.5 cm yr^{-1} is used as minimum value. In data sparse areas, the standard deviation of the ERS-2 data within one RACMO2/ANT grid cell is weighted with the area without data. This produces higher $\sigma_{ERS\text{-}2}$ values in areas with poor spatial sampling (Fig. S9h).

The root-sum-square of $\sigma_{ERS\text{-}2}$ and $\sigma_{firndepth}$ yields the overall error in dH/dt_{corr} (σ_{corr}, Fig. S9i). The ratio of dH/dt_{corr} with σ_{corr} (Fig. S9j) shows that thinning rates in the ASE and thickening rates in continental East Antarctica are significant. On the other hand, thickening rates in coastal WL are not significant. Error bars on the elevation change estimates in Fig. 3 in the manuscript are the product of the root-sum-square of $\sigma_{firndepth}$

(green bars), $\sigma_{ERS\text{-}2}$ (blue bars) and σ_{corr} (red bars), and have a length of 2σ corresponding to 95% confidence interval).

The error on the value of ρ_1 can be calculated from contributions of $\sigma_{\rho s}$, σ_β, σ_{acc} and σ_{rc_acc}. Only the contribution from errors in surface density ($\sigma_{\rho s}$, Fig. S9k) and in β (σ_β, Fig. S9l) are shown, the other two are insignificant. However, taking into account these errors does not take into account all the uncertainty regarding firn density, since it is not evident that ρ_1 is indeed the best density to use in the volume-mass conversion. In principle, any value between the surface density (350 kg m^{-3} is often chosen) and the ice density (917 kg m^{-3}) could be used (e.g. *11*). Error bars on the uncorrected ERS-2 dM/dt estimates (blue bars in Fig. S7) are therefore based on these values. For the volume-mass conversion of corrected ERS-2 data, we have modelled the density of the firn that accumulated since 1980, which has somewhat narrowed down the uncertainty to any value between the density of the 1980 firn layer and the ice density. The difference between these two (Fig. S9m) is obviously still large for most of the Antarctic interior, and is by far the largest component of the overall error estimate in ρ_1 ($\sigma_{\rho 1}$ is the root-sum-square of $\sigma_{\rho s}$, σ_β, σ_{acc}, σ_{rc_acc} and (ρ_i-ρ_1), Fig. S9n). Note that ρ_i-ρ_1 is the maximum range of densities, so the error in firn density ($\sigma_{\rho 1}$, Fig. S9n) is likely overestimated.

Using the above-mentioned error estimates σ_{corr} and $\sigma_{\rho 1}$, the overall error in mass changes ($\sigma_{dM/dt}$, Fig. S9o) can be calculated for the grounded ice sheet within the region of coverage, under the assumption that the grounded ice area is exactly known. The resulting pattern of $\sigma_{dM/dt}$, clearly shows that large uncertainties in mass estimates exist in coastal areas, which coincides with locations where the elevation change signals are also largest. Especially the AP exhibits large uncertainties in elevation and mass changes.

Choosing ρ_1 for the volume-mass conversion means that resulting mass change is a conservative estimate. Hence, the resulting error is larger on the positive side of the mass estimate. Since we differentiate between ρ_i (drainage basins 14, 15, 16 and 19) and ρ_1 (all other basins) for the volume-mass conversion, different positive and negative error bars are plotted for the mass estimates per drainage basin (Fig. 3b in the manuscript). These error bars are derived from the root-sum-square of $\sigma_{dM/dt}$, computed per drainage basin, resulting in typical uncertainties for mass changes per drainage basin. The error bars have a length of 2σ (corresponding to 95% confidence interval).

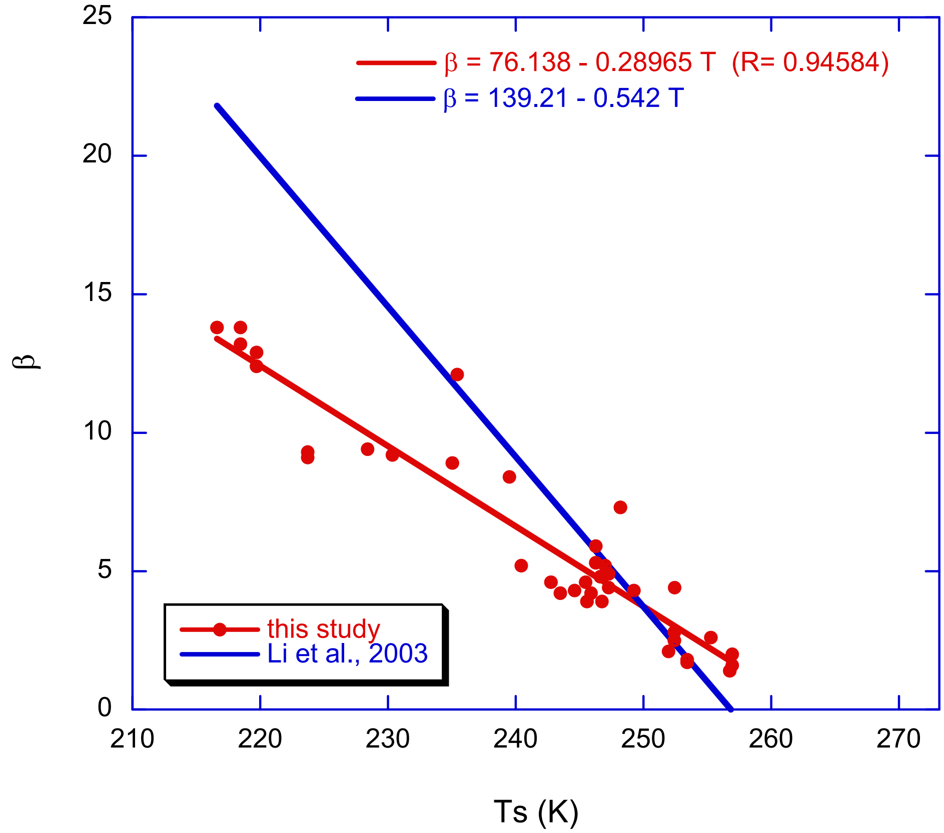

Fig. S1: Values of β (red dots) as a function of mean surface temperature over Antarctica. The relation of (*S1*) for Greenland is plotted in blue.

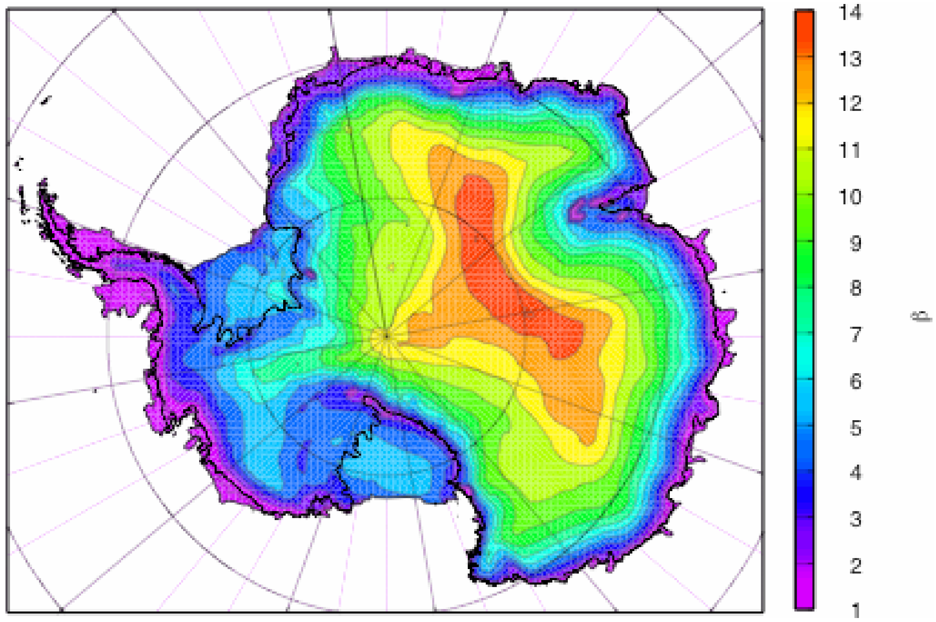

Fig. S2: Distribution of the tuning parameter β over Antarctica, using T_s from RACMO2/ANT.

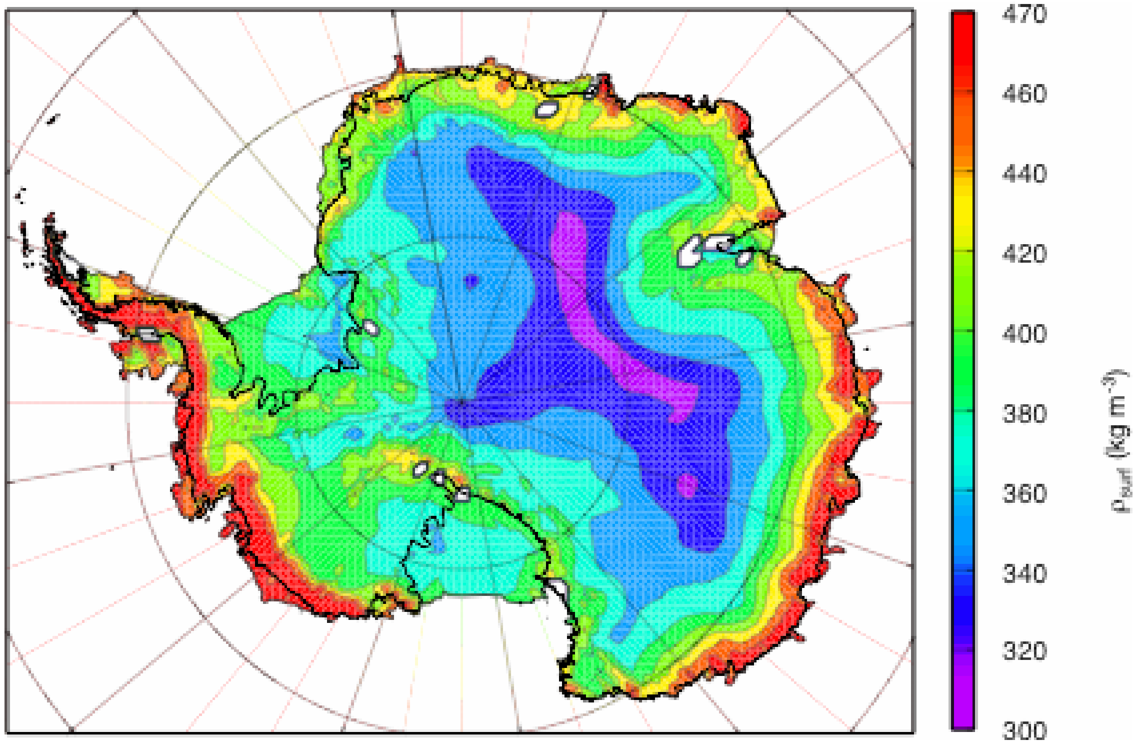

Fig. S3: Simulated surface density (ρ_s) resulting from the parameterisation (*S2*) and using temperature, wind speed and annual accumulation from RACMO2/ANT (*20*).

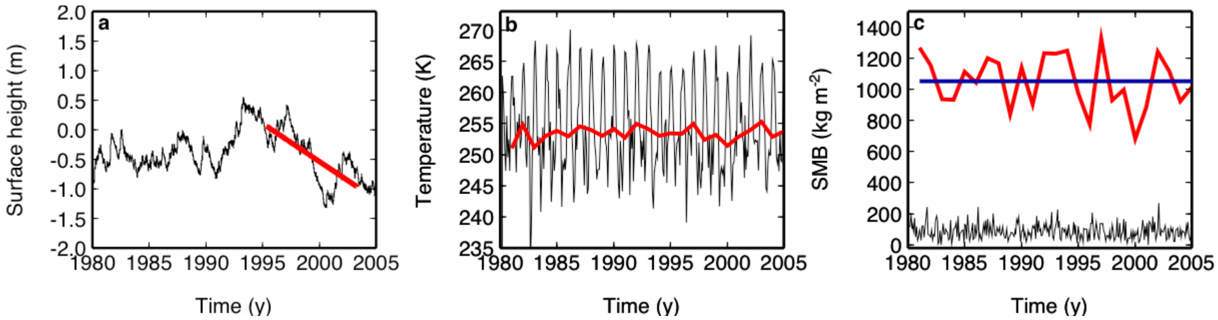

Fig. S4: Simulated firn depth change (a) for Law Dome, and associated monthly and annual values of temperature (b) and accumulation (c).

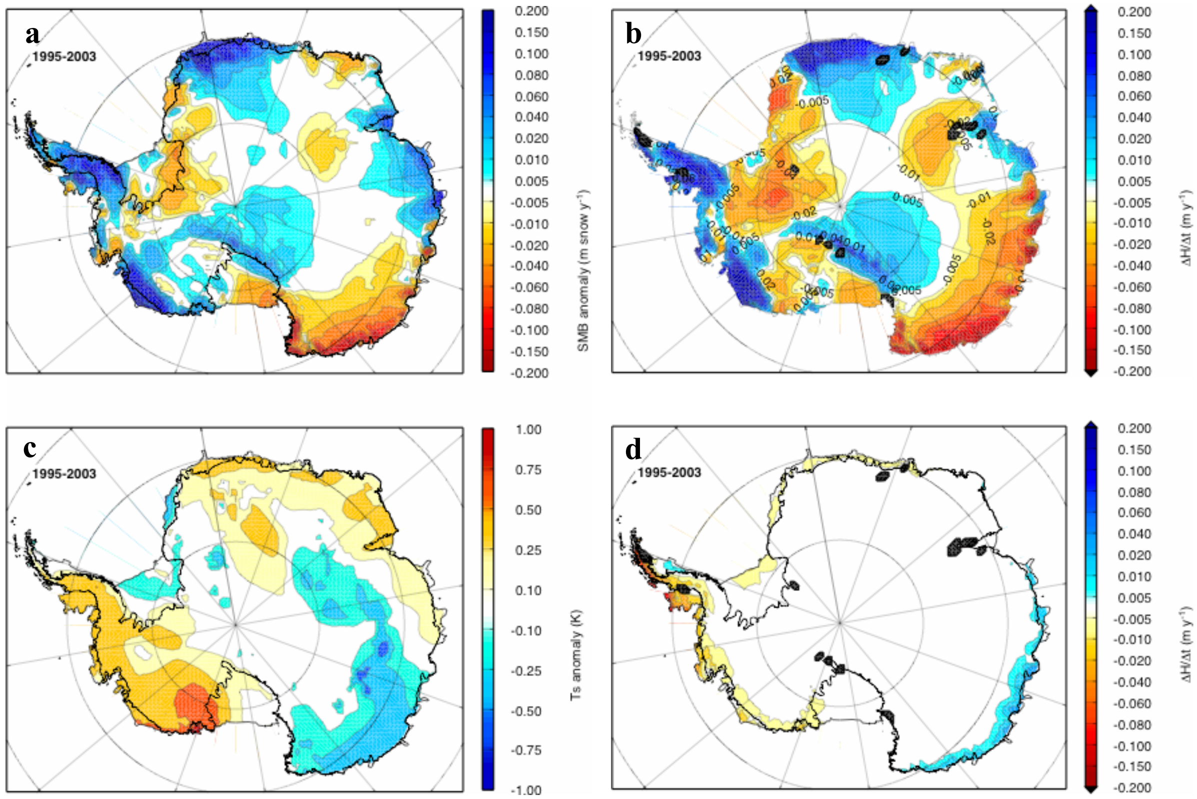

Fig. S5: Anomaly in accumulation (a) and temperature (c) in the period 1995-2003 (relative to the 1980-2004 mean), and resulting firn depth trends over the period 1995-2003 in model runs that are forced by either time-dependent accumulation rate and constant temperature (b) or constant accumulation rate and time-dependent temperature (d).

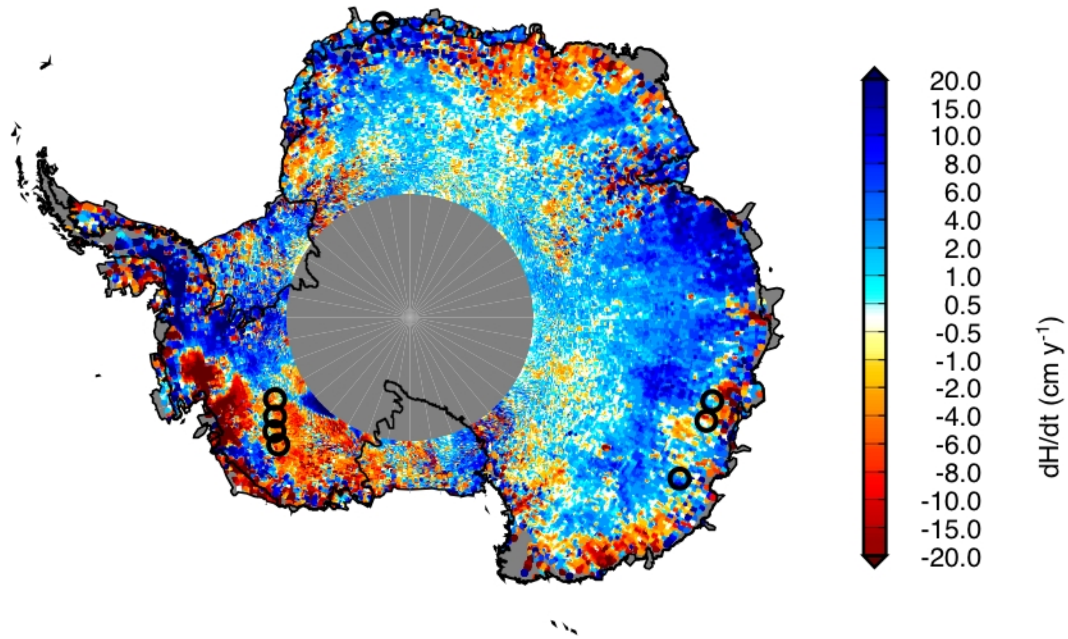

Fig. S6: Observed (ERS-2) surface elevation trends over the period 1995-2003. Circles indicate the location of ice cores used for the accumulation records in Fig. 1.

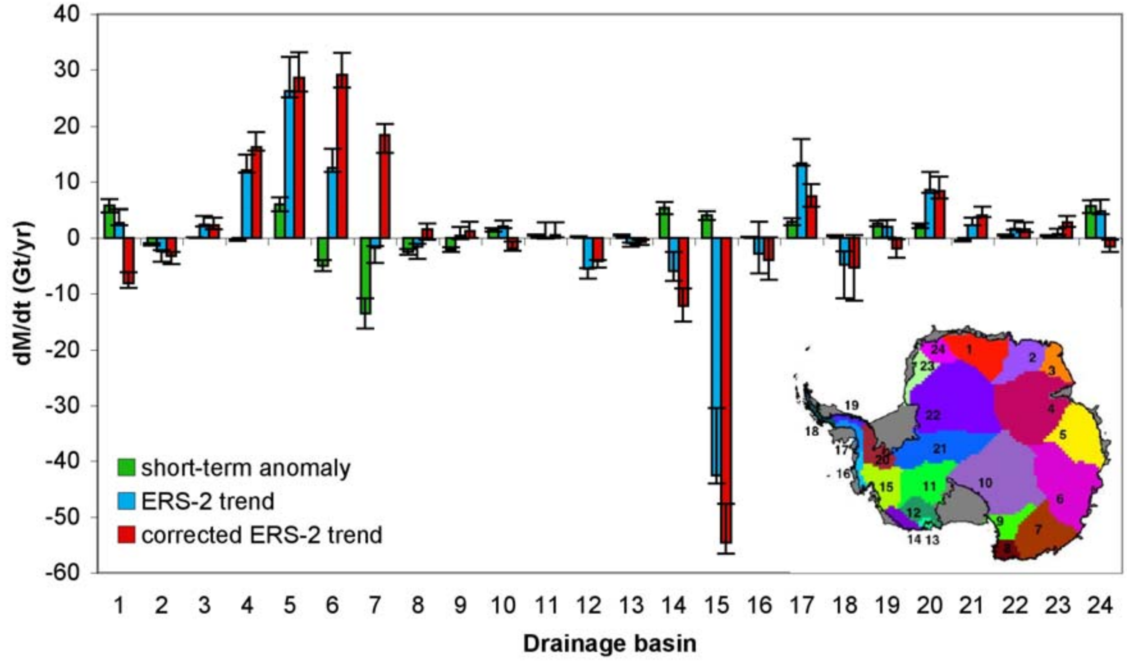

Fig. S7: Mass changes per drainage basin, with a distinction between contributions of short-term accumulation anomalies (1995-2003 relative to 1980-2004, green bars), the original ERS-2 estimates (1995-2003, blue bars) and the trends computed from ERS-2 data corrected for the 1995-2003 firn depth effects (red bars = blue - green). Drainage basin 15 clearly suffers from severe mass loss, whereas 4 drainage basins in WL evidently are gaining mass.

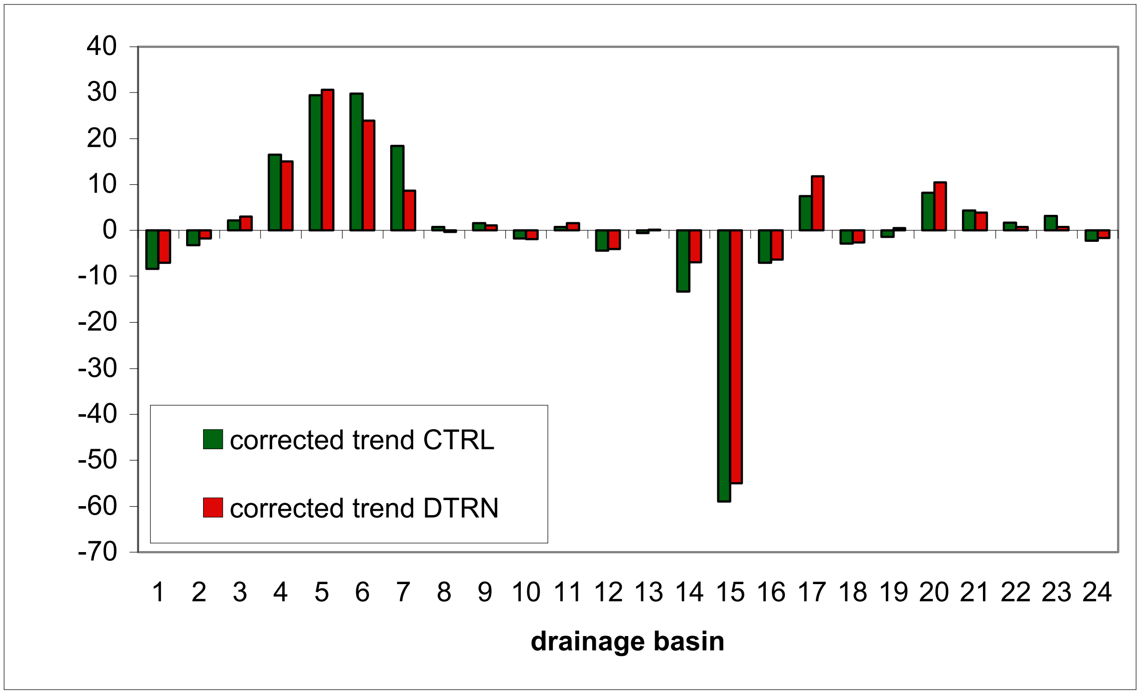

Fig. S8: Mass changes per drainage basin due to long-term trends in accumulation (1980-2004 relative to accumulation rate that balances vertical ice velocity), with a distinction between the control simulation (CTRL) and the simulation using the de-trended accumulation (DTRN).

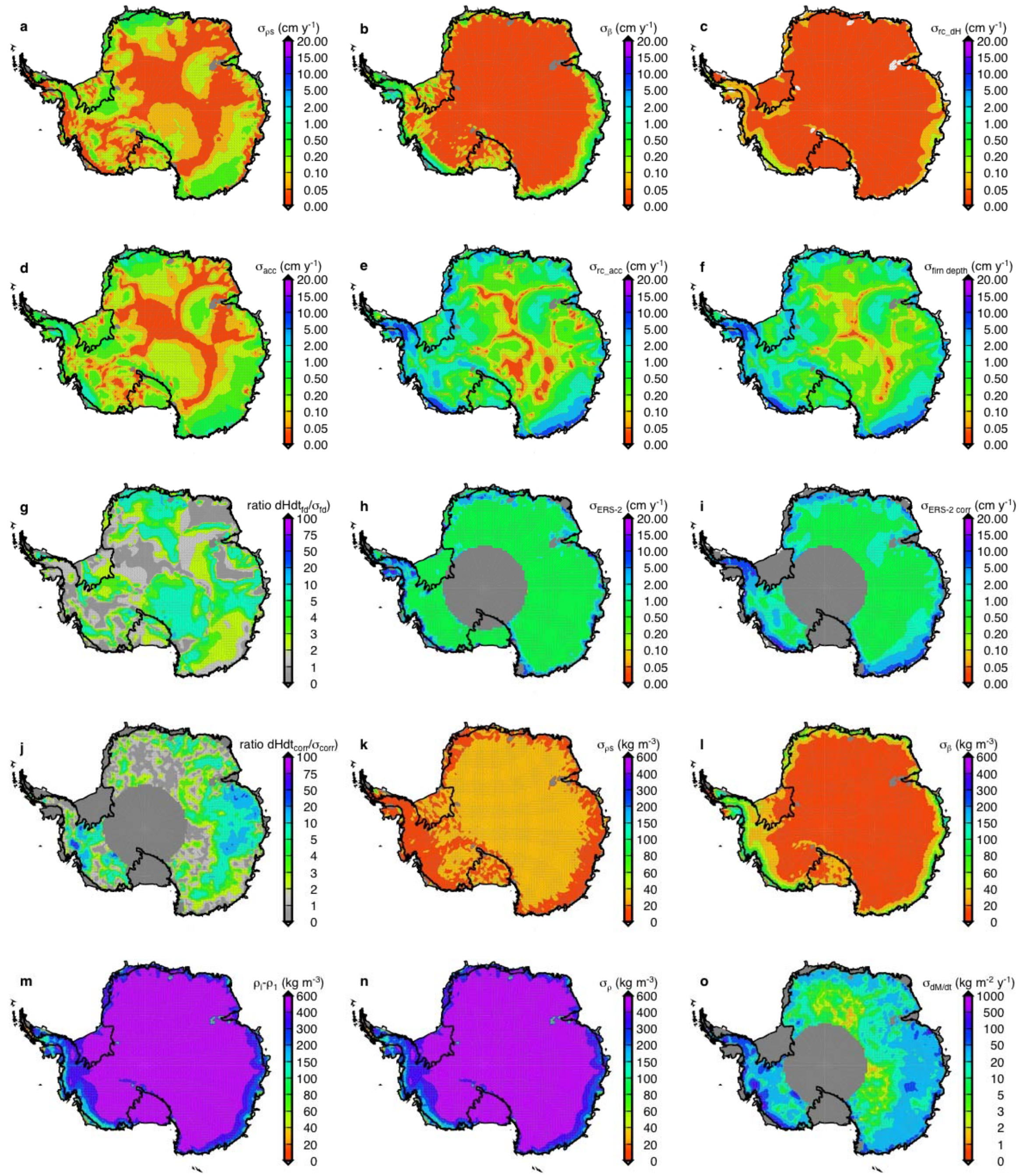

Fig. S9: Different components of error estimates in the analysis presented in this study. Individual error estimates in simulated firn depth change (1995-2003) due to uncertainties in ρ_s (a), densification tuning parameter β (b), regression coefficient of trend through simulated dH time series (c), mean annual accumulation (d) and 25yr trends in accumulation time series (e) result in the total error estimate in simulated firn *depth change (f). The ratio of simulated firn depth change with its error is shown in (g) and reveals areas where simulated firn depth changes are significant. The error in ice sheet elevation change from ERS-2 (h) is combined with (f), which yields the error in ice sheet elevation change corrected for 1995-2003 firn depth changes (i). The ratio of these corrected elevation change with its error is shown in (j). When the ratio>2, elevation change results are significant (95% confidence). Individual error estimates in firn density due to uncertainties in* ρ_s *(k), densification tuning parameter* β *(l), difference between* ρ_i *and* ρ_I *(m) produce an overall error estimate in firn density (n). The resulting overall error in mass changes (o) is computed from (i) and (n), and is largest in coastal areas, and especially in the AP.*

Table S1: Mass change rates per area, covering in total 94 10^6 km^2 (78% of total grounded ice sheet area).

	Mass changes [Gt yr^{-1}]		
	95-03 Acc anomaly	Uncorrected ERS-2	Corrected ERS-2
ASE	10 ±1	-51 ±14	-71 ±9
Rest WA	9 ±1	15 ±9	8 ±8
EA	-5 ±4	60 ±10	87 ±9
Total	14 ±4	24 ±19	25 ±14

References

S1. J. Li, H.J. Zwally, H. Cornejo, D. Yi, *Ann. Glaciol.* **37**, 233 (2003).

S2. K. Kaspers *et al.*, *Atmos. Chem. Phys.* **4**, 1365 (2004).

S3. W.S.B. Paterson, *The physics of glaciers* (Butterworth-Heinemann, Oxford, 1994) 496p.

S4. G. Robin, *The climatic record in polar ice sheets,* 180 (1983).

S5. E. Rignot, *Phil. Trans. R. Soc. A Math. Phys. Eng. Sci.* **364**, 1637 (2006).

S6. G. Ramillien *et al.*, *Global Planet. Change* **53**, 198 (2006).

S7 J.L. Chen, C.R. Wilson, D.D. Blankenship, B.D. Tapley, *Geophys. Res. Lett.* **33**, L11502 (2006).